



Ice surface near melting point: Effects on the tropospheric ice

Guillermo Aguirre VARELA^{1,2*} , Carlos L. Di PRINZIO^{1,2} 
and Damián STOLER¹ 

¹FAMAF, Universidad Nacional de Córdoba, Medina Allende and Haya de la Torre,
5000 Ciudad Universitaria, Córdoba, Argentina

²IFEG-CONICET, Universidad Nacional de Córdoba, Medina Allende and Haya
de la Torre, 5000 Ciudad Universitaria, Córdoba, Argentina

* corresponding author <g.aguirre.varela@unc.edu.ar>

Abstract: Atmospheric gases and chemical impurities can be stored and chemically transformed in the tropospheric ice. Impurities are rejected during freezing of the ice to the grain boundaries, free ice surfaces or inclusions. Surface snow and tropospheric ice, however, may be exposed to high temperatures and, eventually, the gases and chemical impurities can be released into the environment. It is important to study the surface structure and transport mechanisms at temperatures near the melting point because the location of impurities and their interactions with water molecules in the ice are not yet sufficiently explained. In this work, the evolution of a scratch on the bicrystalline ice surface was studied at -5°C . The surface transport mechanisms near the melting point were studied and, as a consequence, the surface structure could be determined. An ice sample was kept immersed in ultra-pure silicone oil to prevent evaporation and, thus, isolate the effect of surface diffusion. The ice sample was made with water with chemical conditions similar to the water of polar ice sheets. Photographs of the scratch were taken periodically, for approximately 50 hours, using a photographic camera coupled to an optical microscope. From these images, the evolution of the width of the scratch was studied and the surface diffusion was the dominant transport mechanism in the experiment. Finally, the ice surface self-diffusion coefficient at -5°C was determined and it was very similar to the super-cooled water diffusion coefficient. A liquid-like behavior of ice surfaces near the melting point was found and it could have a strong influence on the reaction rates with atmospheric gases.

Keywords: ice self-diffusion coefficient, air-ice interaction, quasi-liquid layer, surface transport mechanisms.



Introduction

In nature, ice is found in snow, hail, glaciers and polar ice sheets (Hobbs 2010). Ice absorbs many natural and anthropogenic gases that contribute to global warming effect (Raynaud *et al.* 1993). Gases are preferably absorbed on the surface of the ice (Bar-Nun *et al.* 1987; Krausko *et al.* 2014).

Bartels-Rausch *et al.* (2014) studied the interaction of impurities with snow and ice. It was shown that the physical processes of impurities vary significantly depending on their location in the ice and the ice surface structure. These authors present the studies of the ice surface properties and the new experimental techniques. However, the chemical reactions and physical processes, inside and outside the snow grains, are not yet sufficiently analyzed. The ice surface structure changes with the physical conditions (Pruppacher *et al.* 2010) and the liquid-like behavior of ice surfaces near the freezing point can strongly modify the chemical reaction rates with ice. The ice surface structure and its effects on the surface diffusion processes of contaminants could be very useful in atmospheric physics.

Dash *et al.* (2006) showed the ice properties near the melting point and its effects on the environment. Ice melting can start at three types of interfaces: surface melting between a solid and its vapor or gaseous atmosphere, interfacial melting in contact with foreign solids or liquids, and the grain boundary (GB) melting between crystals of the same material. They presented a thermodynamic model of the transition of the interfaces near the melting point. The authors strongly emphasized the importance of the change of the surface structure near the melting point on geophysics. Gas and impurities absorption depends strongly on the surface structure and the transport mechanisms that are activated on the surface (Wettlaufer 1999; Wettlaufer *et al.* 2006; Nasello *et al.* 2007, 2011).

Physical processes in the matter transport that have been studied in relation to GB groove or scratches on surfaces are: evaporation and condensation, surface diffusion, and volumetric diffusion into the solid and gaseous environment surrounding the sample (Mullins 1957, 1959, 1960; King *et al.* 1962; Gruber *et al.* 1966; Nasello *et al.* 2007, 2011).

Bartels-Rausch *et al.* (2013) evaluated the structure of the snow pack, the interaction of trace gases with the snow surface and the ice grain boundaries. The observed diffusion profiles could be well described based on gas-phase diffusion and the known structure of the snow sample at temperatures $\geq -20^{\circ}\text{C}$.

Mullins (1957) studied the mass transport by evaporation and condensation corresponding to a GB groove in contact with its vapor. Finally, he completed the work by studying the diffusive transport on the surface of the solid, without the presence of fluid and controlled by the local curvature of the surface. Mullins (1960) studied the GB groove taking into account the effect of the curvature of the surface in contact with the gas and, therefore, the changes in the vapor densities. He also considered the volume diffusion in the same work. Later, King *et al.* (1962) analyzed the evolution of a superficial scratch considering the simultaneous

mechanism of surface and volume diffusion. Gruber *et al.* (1966) reported a surface flattening analysis considering the effects of surface and volumetric diffusion taking into account the asymmetry of the structures evolving on the surface.

In order to describe the evolution of a scratch on the surface of a solid, Mullins (1959) assumed the presence of a viscous fluid and used the Navier-Stokes equations to find the transport equations. He also considered the effect of surface curvature and proposed a surface diffusion model, similar to that proposed in Mullins (1957) to describe the evolution of the emerging groove of a grain boundary. Furthermore, he considered other transport mechanisms related to gaseous diffusion and volumetric diffusion that could be influencing the evolution of the surface scratch.

Style *et al.* (2005) presented a transport model considering the presence of a quasi-liquid layer on the surface. They studied the transport of matter on the quasi-liquid surface using thermodynamic arguments (Dash *et al.* 2006). They applied this model to describe the evolution of a GB groove in an environment with high vapor pressure, obtaining Mullins' equation (Mullins 1959) in an asymptotic way.

Asakawa *et al.* (2016) carried out studies of the ice surface and reported the presence of two types of quasi-liquid layers with different morphologies. Both types of layers are present only if the vapor pressure is higher than a given critical value and at temperatures close to melting point. According to these authors, the quasi-liquid layers control the surface properties of ice just below the melting point. It is well known that ice surface melting governs a wide variety of phenomena, such as ice growth and its interaction with gases and atmospheric pollutants.

In this work, the evolution of an ice surface scratch is presented to study the surface transport mechanisms and the ice surface structure. In this way, gas transportation on ice surface could be explored because it changes dramatically near the melting point (Bartels-Rausch *et al.* 2014). The self-diffusion coefficient of pure ice surface was determined by studying the width evolution of a surface scratch. The scratch width was determined by photographs directly from the surface of a bicrystalline ice sample at -5°C . A theoretical surface model was fitted to the experimental data and the surface diffusion mechanism was revealed. The surface self-diffusion coefficient of the ice surface was obtained and it was compared with the experimental results obtained by other authors.

Material and methods

A bicrystalline ice sample was used in these experiments and the sample surface was polished with a microtome in a cold chamber at -10°C . The bicrystal was made according to the experimental method reported by Nasello *et al.* (1992, 2007, 2011) and Di Prinzio *et al.* (1997). The ice sample was placed on a microtome plate as shown in Fig. 1A.

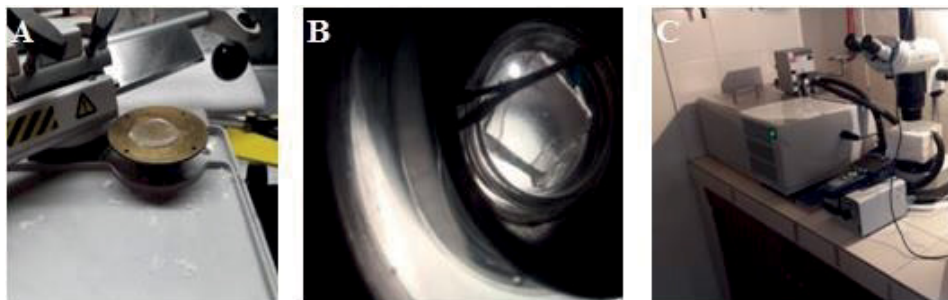


Fig. 1. Ice sample on the microtome stage (A), ice sample in the acrylic transparent cell with silicon oil (B) and experimental set-up of microscope with digital camera controlled by computer and cold cell thermostatically controlled by the LAUDA® circulating bath (C).

The bicrystal was made using ultra-pure water obtained from Milli-Q® filter with $0.6 \mu\text{S}$ conductivity and impurities concentration less than 10 ppb (Nasello *et al.* 1992, 2007, 2011; Di Prinzio *et al.* 1997). The sample was made under the same conditions of impurities and conductivity recorded in the water of polar ice in surface layers (Palais *et al.* 1985; Durand 2006) in order to compare the experimental results with those presented in natural ice.

A scratch pattern was made on the surface with a metal blade with triangular-tipped teeth and the ice sample was immediately immersed in a transparent cell with pure silicon oil (Fig. 1B). The depth and width of the blade teeth were similar (approximately $10 \mu\text{m}$).

The acrylic cell was sealed and placed into a cold box thermostatically controlled by a circulating bath LAUDA® at $-5 \pm 1^\circ\text{C}$ (Fig. 1C). This initial setup procedure took approximately 45 minutes (t_0). The evolution of the surface scratches was registered for approximately 50 hours by periodic photographs obtained with a digital camera attached to an optical microscope (Olimpus®). Photographs of the surface scratches were taken every 15 minutes.

Analysis of the photographs

The photographs were converted from color to grey tones. Figure 2A shows the surface of the bicrystalline sample, the grain boundary (GB) and the stripes. The GB is horizontal, the scratches are vertical and a wider central scratch was used in this study.

In order to determine the surface plane on both sides of the GB, the procedure developed by Higuchi (1957) was carried out. A plastic replica of the surface of an ice crystal allows the crystalline disorientation of the sample to be determined. The ice crystal must remain during the whole process in a cold chamber around -10°C and its surface must be properly polished by a microtome. An airtight container with silica gel crystals should be located inside the working chamber. After the polished process, the sample is allowed to relax inside the silica

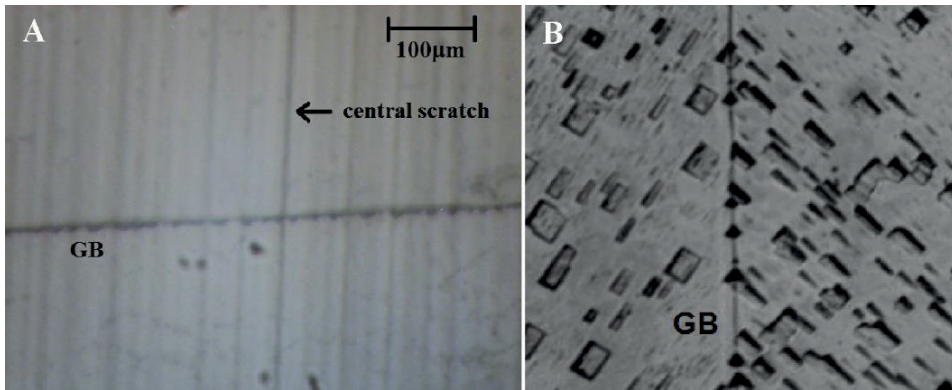


Fig. 2. Grain boundary and vertical central scratch considered in this study (A) and plastic replica with the etch pits (B).

container for 5 minutes. The sample is taken out of the container and the surface is covered with a very thin layer of a solution of formvar® at 1% in 1,2-dichloroethene. The sample is placed back in the airtight container for 10 minutes. The 1,2-dichloroethene evaporates quickly producing micropores on the plastic surface, and due to the dry air, the ice surface sublimates through this holes (Nasello 1982). This sublimation is conditioned by the crystal structure, leading to the pits formation copying the crystal structure. After 10 minutes, a thick layer of a formvar® solution at 4% in 1,2-dichloroethene is added all over the surface. The pits are filled with the solution and the ice sublimation process is stopped. The sample is stored in the container with silica gel until the following day, allowing the plastic surface to dry completely. Finally, a negative copy of the original pits formed due to sublimation was obtained.

Figure 2B shows a plastic replica of the bicrystalline sample presenting the thermal etched pits that serve to determine the surface plane on both sides of the GB (Higuchi 1957). Clearly, both crystalline planes are slightly different and very close to the plane $(1\ 0\ \bar{1}\ 0)$.

The grey profiles of the central scratch, corresponding to the crystalline plane on both sides of the GB and for each photograph, were obtained using the free software ImageJ® (Abràmoff *et al.* 2004). Barletta *et al.* (2012) estimated the vein volume within the Greenland and Antarctic ice sheets in a calibrated photograph using ImageJ.

Figure 3A shows an example of the grey profile and the average illumination curve. The average background lighting was subtracted from the grey profile to study the evolution of the width of the central scratch. Figure 3B shows the corrected grey profile. The central minimum corresponds to the central scratch under study. The pixel-mm equivalence was established in the photographs, using a 100 μm scale with an appreciation of 5 μm.

The width of the central scratch $a(t)$ was considered the dark area. In order to determine the width, the distance between the two “points” (see Fig. 3B) that

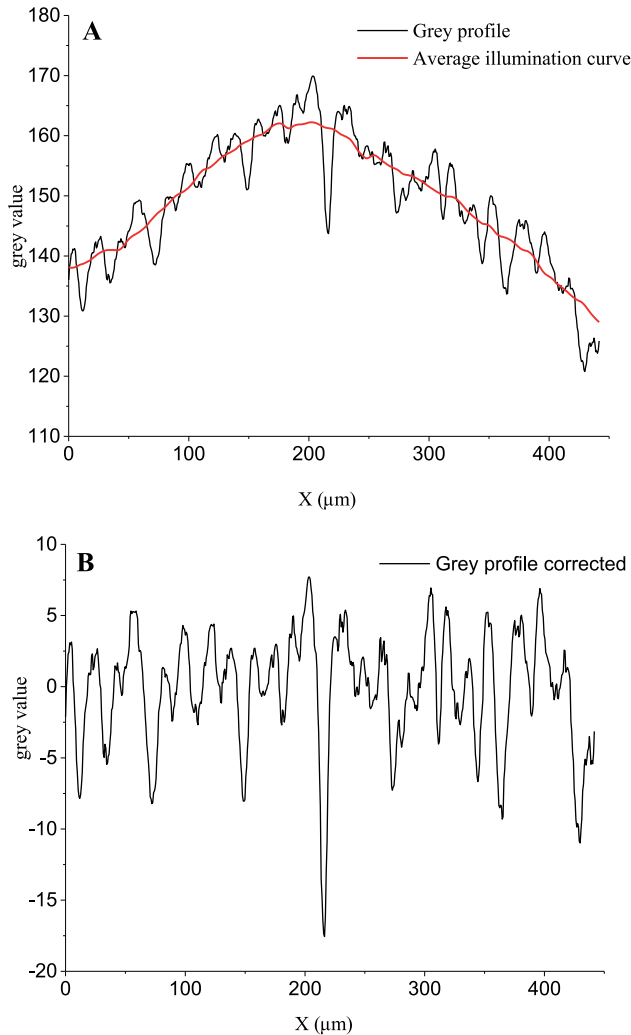


Fig. 3. Grey profile for a region above the grain boundary (A) and previous grey profile corrected for average lighting background (B). The horizontal axis shows the position along a horizontal line of the photo. The vertical axis shows the correspondent mean grey value.

define the edge of the dark area was considered (Abràmoff *et al.* 2004; Barletta *et al.* 2012). This was done using the corrected grey profiles. In this way, the temporal evolutions of the width of the central scratch on the crystalline plane on both sides of the GB were determined.

Results

The widths of the central scratch $a(t)$ were calculated on both sides of the GB (Region 1 and 2). The experimental results were presented in Fig. 4.

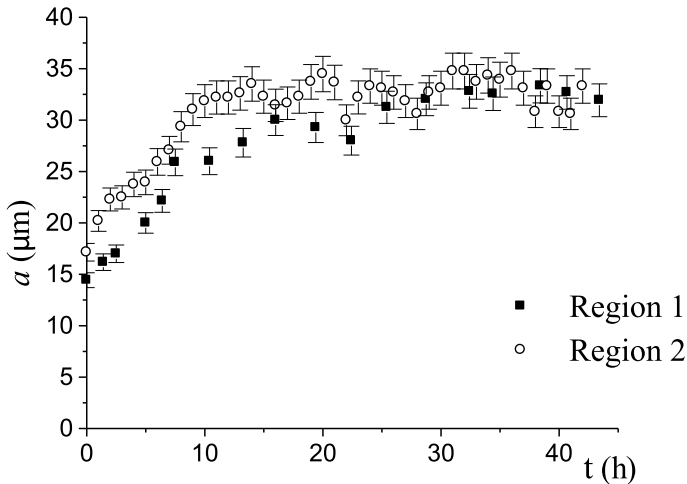


Fig. 4. Temporal evolution of $a(t)$ for each region. The time is represented in the horizontal axis and the width of the central scratch is reported in the vertical axis.

The widths and time are normalized with the initial values corresponding to the first photograph. The natural logarithms of the normalized quantities are presented, and a linear fit is shown in Fig. 5. The linear equation is represented by:

$$\text{Ln}\left(\frac{a^i}{a^i_0}\right) = k^i \text{Ln}\left(\frac{t}{t_0}\right) + f^i \quad (1)$$

where a^i is the width of the central scratch in Region i (1, 2) at time t , a^i_0 is the first measured value in Region i at time t_0 . Table 1 shows the coefficients (k^1, f^1) corresponding to the fit in the Region 1 and (k^2, f^2) corresponding to the fit in the Region 2. Both coefficients f^i are indistinguishable from zero, while the slopes are indistinguishable from each other. We could describe the variation of the central scratch width with time, both in Region 1 and in Region 2 (Fig. 2), by the following equation

$$a^i(t) = a^i_0 \left(\frac{t}{t_0}\right)^{k^i} \quad (2)$$

Table 1.

Coefficients (k^i, f^i) and – squared of regions 1 and 2 using equation (1).

	Coefficients	R ²
k^1	0.23 ± 0.02	0.8981
f^1	-0.04 ± 0.06	
k^2	0.22 ± 0.01	0.9214
f^2	0.01 ± 0.03	

Discussion

The width of the central scratch follows a power law in time for each region. Furthermore, since k^i are indistinguishable from each other, the evolution of the central scratch on the crystalline planes on both sides of the GB seems to be controlled by the same physical process. As the experiments were carried out with the surface of the ice covered with a layer of silicon oil, the mass transport that flattens the central scratch was caused by surface diffusion.

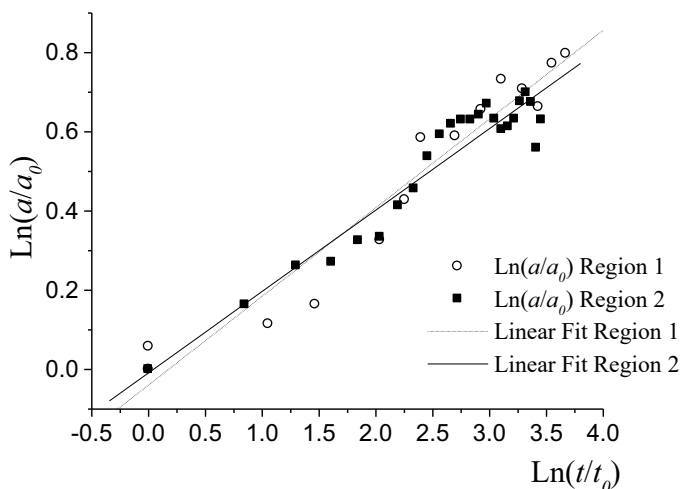


Fig. 5. Natural logarithms of $\left[\frac{a}{a_0}\right]$ versus natural logarithms of $\left[\frac{t}{t_0}\right]$ are presented (circles for Region 1 and squares for Region 2) and the correspondent linear regression fits for each region.

The presence of a quasi-liquid layer on the ice surface has been reported in numerous studies. In particular, Asakawa *et al.* (2016) reported two types of quasi-liquid layers with different morphologies only present in conditions of high vapor pressures and temperatures $> -3^\circ\text{C}$. However, it occurs when the surface of the ice is in contact with its vapor.

In our case, the quasi-liquid layer is between two mediums: solid ice on one side and silicone oil on the other. Style *et al.* (2005) and Dash *et al.* (2006) reported a similar law with exponent $1/4$, which is close to the values of k^i found in the present work. This would indicate that the diffusion process in our experiments would have a behavior similar to the one expected on the surface of ice with quasi-liquid layer, since it has the same power law.

The model proposed by Style *et al.* (2005) to describe the quasi-liquid layer is not restricted only to situations where the quasi-liquid layer is in contact with a gaseous medium. It can be seen that the effect of another substance above the quasi-liquid layer could be taken into account in the free energy of the quasi-liquid layer-substance interface. In this sense, it would be possible to use the proposed "quasi-liquid layer" model to analyze our results. The experimental

results respond to a similar power law and the exponents corresponding to each zone are indistinguishable from the power law reported by Style *et al.* (2005).

In order to compare the results, the transport coefficient B corresponding to each zone was estimated using the parameters of the fits. The power law proposed by Style *et al.* (2005) and the power law proposed by Mullins (1959) were used to calculate the theoretical transport coefficients predicted by each model. Thus

$$a_{teo} = 5.7 (Bt)^{1/4} \quad (3)$$

Rewriting the equation (3) with the coefficients and values corresponding to one hour from the start of the experiment, the following is obtained:

$$\frac{a_0^i}{3600^{k^i}} = 5.7 (B_i)^{1/4} \quad (4)$$

Values of B_i were determined, which are presented in Table 3.

Style *et al.* (2005) found an expression for B in terms of liquid water properties and melting temperature and they obtained a value of B considering the sample in contact with air and at a temperature of -1°C . However, in our experiment, the interface was ice-water-silicone oil.

Using the physical parameters corresponding to our experiment (see Table 2) and the expression found by Style *et al.* (2005), the value calculated was $B \sim 3 \cdot 10^{-28} \text{ m}^4 \text{ s}^{-1}$. This value of B is similar to those obtained in this experimental work and presented in Table 3.

On the other hand, using the values of the transport coefficient B obtained in this work, the physical parameters (Table 2), and the functional form for the

Table 2.

Experimental values measured for physical parameters for pure ice.

Physical parameters for pure ice	Experimental values	References
the molar volume of diffusing species	$3.6 \cdot 10^{-29} \text{ m}^3$	Hobbs (2010)
number of molecules per unit of area	$3.29 \cdot 10^{18} \text{ m}^{-2}$	Hobbs (2010)
silicon oil-liquid surface energy	0.03531 Jm^{-2}	Gu (2001)
liquid-solid surface energy	0.033 Jm^{-2}	Hobbs (2010)
Hamaker constant	$0.3 \cdot 10^{-20} \text{ J}$	Gu (2001)
melting point	273 K	Hobbs (2010)
dynamic viscosity of water	0.00216 Pa	Hallet (1963)
density	999.7 Kgm^{-3}	Hallet (1963)
latent heat of fusion	334000 JKg^{-1}	Hobbs (2010)

transport coefficient B proposed by Mullins (1959), two “self-diffusion coefficients” D_i (associated to each B_i) were determined. The results are presented in Table 3.

Table 3.

Transport coefficient and “self-diffusion coefficients” (associated with each).

$B_1 \cdot (\text{m}^4 \text{s}^{-1})$	$(3.3 \pm 0.4) 10^{-28}$
$D_1 \cdot (\text{m}^2 \text{s}^{-1})$	$(2.6 \pm 0.4) 10^{-9}$
$B_2 \cdot (\text{m}^4 \text{s}^{-1})$	$(1.2 \pm 0.7) 10^{-28}$
$D_2 \cdot (\text{m}^2 \text{s}^{-1})$	$(1.0 \pm 0.3) 10^{-9}$

The values of D_i are different, and this could be associated with the different crystalline structures of the surface planes, which can have in general different physical properties (Nasello *et al.* 2007, 2011; Druetta *et al.* 2013; Di Prinzio *et al.* 2016). We can say that both values of surface diffusion coefficient found in this work and the values by Nasello *et al.* (2011) are comparable to the value $3 \times 10^{-9} \text{m}^2 \text{s}^{-1}$ of the coefficient of water self-diffusion at atmospheric pressure and at -5°C reported by Guevara *et al.* (2011).

Finally, it would be possible to think that the “liquid layer” model proposed to analyze our results was correct. For historical reasons, most studies of ice surface focused on temperatures relevant to the stratosphere or the upper troposphere. Surface snow and tropospheric ice, however, may be exposed to warmer conditions. The atmospheric gas absorption processes are affected by the structure of the ice surface, and the liquid-like behavior of ice surfaces near the freezing point can strongly modify the absorption of gases in ice (Bartels-Rausch *et al.* 2014).

The experimental method presented in this work is based on the study of the evolution of a scratch on the ice surface and shows that the ice surface near the melting point has liquid-like behavior. Moreover, the results were similar to the coefficient of self-diffusion of supercooled water at atmospheric pressure. Therefore, the experimental method developed in this work would allow us to study the surface self-diffusion coefficient of ice at different temperatures, between -2°C and -15°C according to our experimental setup, with different conditions of impurities, and with different surface crystalline planes.

Conclusion

We presented an experimental method to find the ice surface diffusion coefficient. The method is based on the study of the evolution of a scratch on the ice surface. The surface diffusion coefficient of ice on the crystalline plane

(1 0 $\bar{1}$ 0) was determined experimentally for -5°C . Our results are in good accord with the values reported by Nasello *et al.* (2011). We found results consistent with the presence of a liquid like layer on the ice surface near the melting point.

Acknowledgements. – This work was possible thanks to the collaboration with José Barcelona from IFEG-CONICET. The financial support was given by SeCyT (UNC's Secretariat for Science and Technology) and CONICET (Consejo Nacional de Investigaciones Científicas y Técnicas de Argentina). Special thanks to the anonymous reviewers who have made very important suggestions and contributions to this article.

References

- ABRÀMOFF M.D., MAGALHÃES P.J. and RAM S.J. 2004. I processing with ImageJ. *Biophotonics International* 11: 36–42.
- ASAKAWA H., SAZAKIGI., NAGASHIMA K., NAKATSUBO S. and FURUKAWA Y. 2016. Two types of quasi-liquid layers on ice crystals are formed kinetically. *Proceedings of the National Academy of Sciences* 113: 1749–1753.
- BARLETTA R.E., PRISCU J.C., MADER H.M., JONES W.L. and ROE C.H. 2012. Chemical analysis of ice vein microenvironments: II. Analysis of glacial samples from Greenland and Antarctica. *Journal of Glaciology* 58: 1109–1118.
- BAR-NUN A., DROR J., KOCHAVI E. and LAUFER D. 1987. Amorphous water ice and its ability to trap gases. *Physical Review B* 35: 2427.
- BARTELS-RAUSCH T., WREN S.N., SCHREIBER S., RICHE F., SCHNEEBELI M. and AMMANN M. 2013. Diffusion of volatile organics through porous snow: impact of surface adsorption and grain boundaries. *Atmospheric Chemistry and Physics* 13: 6727–6739.
- BARTELS-RAUSCH T., JACOBI H.W., KAHAN T.F., THOMAS J.L., THOMSON E.S., ABBATT J.P., AMMANN M., BLACKFORD J.R., BLUHM H., BOXE C. and DOMINÉ F. 2014. A review of air–ice chemical and physical interactions (AICI): liquids, quasi-liquids, and solids in snow. *Atmospheric Chemistry and Physics* 14: 1587–633.
- DASH J.G., REMPEL A.W. and WETTLAUFRER J.S. 2006. The physics of premelted ice and its geophysical consequences. *Reviews of Modern Physics* 78: 695.
- DI PRINZIO C.L. and NASELLO O.B. 1997. Study of grain boundary motion in ice bicrystals. *The Journal of Physical Chemistry* 39: 7687–7690.
- DI PRINZIO C.L. and PEREYRA R.G. 2016. Molecular dynamics simulations of tilt grain boundaries in ice. *Modelling and Simulation in Materials Science and Engineering* 24: 045015.
- DRUETTA E., NASELLO O.B. and DI PRINZIO C.L. 2013. Experimental Determination of $\langle 1010 \rangle / \Psi$ Tilt Grain Boundary Energies in Ice. *Journal of Materials Science Research* 3: 71–76.
- DURAND G., WEISS J., LIPENKOV V., BARNOLA J.M., KRINNER G., PARRENIN F., DELMONTE B., RITZ C., DUVAL P., RÖTHLISBERGER R. and BIGLER M. 2006. Effect of impurities on grain growth in cold ice sheets. *Journal of Geophysical Research: Earth Surface* 111: F01015.
- GRUBER E.E. and MULLINS W.W. 1966. Extended Analysis of Surface Scratch Smoothing. *Acta Metallurgica* 14: 397–403.
- GU Y. 2001. Experimental determination of the Hamaker constants for solid–water–oil systems. *Journal of Adhesion Science and Technology* 15: 1263–1283.
- GUEVARA-CARRION G., VRABEC J. and HASSE H. 2011. Prediction of self-diffusion coefficient and shear viscosity of water and its binary mixtures with methanol and ethanol by molecular simulation. *The Journal of Chemical Physics* 134: 074508.

- HALLET J. 1963. The temperature dependence of the viscosity of supercooled water. *Proceedings of the Physical Society* 82: 1046.
- HIGUCHI K. 1957. A new method for recording the grain-structure of ice. *Journal of Glaciology* 3: 131–132.
- HOBBS P.V. 2010. *Ice Physics*. Oxford University Press, Oxford.
- KING R.T. and MULLINS W.W. 1962. Theory of the decay of a surface scratch to flatness. *Acta Metallurgica* 10: 601–606.
- KRAUSKO J., RUNSTUK J., NEDÉLA V., KLÁN P. and HEGER D. 2014. Observation of a brine layer on an ice surface with an environmental scanning electron microscope at higher pressures and temperatures. *Langmuir* 30: 5441–5447.
- MULLINS W.W. 1957. Theory of Thermal Grooving. *Journal of Applied Physics* 28: 333–339.
- MULLINS W.W. 1959. Flattening of a nearly plane solid surface due to capillarity. *Journal of Applied Physics* 30: 77–83.
- MULLINS W.W. 1960. Grain boundary grooving by volume diffusion. *Transactions of the American Institute of Mining and Metallurgical Engineers* 218: 354–361.
- NASELLO O.B. 1982. *Estudio de las primeras etapas del proceso de acreción*, PhD Thesis, Universidad Nacional de Córdoba, Córdoba (unpublished).
- NASELLO O.B. and DI PRINZIO C.L. 2011. Anomalous effects of hydrostatic pressure on ice surface self-diffusion. *Surface Science* 605: 1103–1105.
- NASELLO O.B., DI PRINZIO C.L. and LEVI L. 1992. Grain boundary Migration in Bicrystals of Ice. In: Maeno N. and Hondoh T. (eds) *Physics and Chemistry of Ice*, Hokkaido University Press, Sapporo, Japan.
- NASELLO O.B., DI PRINZIO C.L. and GUZMÁN P.G. 2007. Grain boundary properties of ice doped with small concentrations of potassium chloride (KCl). *Journal of Physics: Condensed Matter* 19: 246218.
- PALAIS J.M. and LEGRAND M. 1985. Soluble impurities in the Byrd Station ice core, Antarctica: their origin and sources. *Journal of Geophysical Research: Oceans* 90: 1143–1154.
- PRUPPACHER H.R. and KLETT J.D. 2010. *Microstructure of atmospheric clouds and precipitation. In Microphysics of Clouds and Precipitation*. Springer, Dordrecht.
- RAYNAUD D., JOUZEL J., BARNOLA J.M., CHAPPELLAZ J., DELMAS R.J. and LORIUS C. 1993. The ice record of greenhouse gases. *Science* 259: 926–934.
- STYLE W. and GRAE WORSTER M. 2005. Surface Transport in Premelted Films with Application to Grain-Boundary Grooving. *Physical Review Letters* 95: 176102.
- WETTLAUFER J.S. 1999. Impurity effects in the premelting of ice. *Physical Review Letters* 82: 2516.
- WETTLAUFER J.S. and GRAE WORSTER M. 2006. Premelting dynamics. *Annual Review of Fluid Mechanics* 38: 427–452.

Received 13 October 2020

Accepted 30 June 2021